Thin-Film Modified Electrodes with Reconstituted Cellulose-PDDAC Films for the Accumulation and Detection of Triclosan

ARTICLE *in* THE JOURNAL OF PHYSICAL CHEMISTRY C · FEBRUARY 2008

Impact Factor: 4.77 · DOI: 10.1021/jp709783k

8 AUTHORS, INCLUDING:

Karen Edler
University of Bath
114 PUBLICATIONS **1,227** CITATIONS
SEE PROFILE

Daniel Wolverson
University of Bath
162 PUBLICATIONS **1,161** CITATIONS
SEE PROFILE

Elefteria Psillakis
Technical University of Crete
84 PUBLICATIONS **3,251** CITATIONS
SEE PROFILE

Wim Thielemans
University of Leuven
76 PUBLICATIONS **2,247** CITATIONS
SEE PROFILE

Thin-Film Modified Electrodes with Reconstituted Cellulose−PDDAC Films for the Accumulation and Detection of Triclosan

Michael J. Bonné,[†] Karen J. Edler,[†] J. Grant Buchanan,[†] Daniel Wolverson,[‡] Elefteria Psillakis,[§] Matthew Helton,[||] Wim Thielemans,[⊥] and Frank Marken*,[†]

Department of Chemistry, University of Bath, Claverton Down, Bath BA2 7AY, UK, Department of Physics, University of Bath, Claverton Down, Bath BA2 7AY, UK, Laboratory of Aquatic Chemistry, Department of Environmental Engineering, Technical University of Crete, Polytechnioupolis, 73100 Chania-Crete, Greece, Unilever Research & Development Port Sunlight, Quarry Road, East Bebington, Wirral, CH63 3JW, UK, and Driving Innovation in Chemistry and Chemical Engineering (DICE), School of Chemistry and School of Chemical and Environmental Engineering, University of Nottingham, University Park, Nottingham NG7 2RD, UK

Received: October 6, 2007; In Final Form: November 10, 2007

A strategy for the formation of thin reconstituted cellulose films (pure or modified)) with embedded receptors or embedded ion-selective components is reported. Cellulose nanofibril ribbons from sisal of typically 3−5 nm diameter and 250 nm length are reconstituted into thin films of typically 1.5−2.0 μm thickness (or into thicker free-standing films). Cellulose and cellulose nanocomposite films are obtained in a simple solvent evaporation process. Poly-(diallyldimethylammonium chloride) or PDDAC is readily embedded into the cellulose film and imparts anion permselectivity to allow binding and transport of hydrophobic anions. The number of binding sites is controlled by the amount of PDDAC present in the film. The electrochemical properties of the cellulose films are investigated first for the $Fe(CN)_6^{3-/4-}$ model redox system and then for the accumulation and detection of triclosan (2,4,4′-trichloro-2′-hydroxydiphenyl ether, a hydrophobic polychlorinated phenol). Pure nanocellulose thin films essentially block the access to the electrode surface for anions such as $Fe(CN)_6^{3-}$ and $Fe(CN)_6^{4-}$. In contrast, in the presence of cellulose−PDDAC films, accumulation and transport of both $Fe(CN)_6^{3-}$ and $Fe(CN)_6^{4-}$ in electrostatic binding sites occurs (Langmuirian binding constants for both are about 1.2×10^4 mol^{-1} dm^3 in aqueous 0.1 M KCl). Facile reduction/oxidation at the electrode surface is observed. Triclosan, a widely used antifungal and antibacterial polychlorinated phenol is similarly accumulated into cationic binding sites (Langmuirian binding constant about 2.1×10^4 mol^{-1} dm^3 in aqueous 0.1 M phosphate buffer pH 9.5) and is shown to give well-defined oxidation responses at glassy carbon electrodes. With a cellulose−PDDAC film electrode (80 wt % cellulose and 20 wt % PDDAC), the analytical range for triclosan in aqueous phosphate buffer at pH 9.5 is about 10^{-6}−10^{-3} mol dm^{-3}.

1. Introduction

Cellulose is a natural polymer of considerable importance and with a wide range of applications due to its abundance, physical properties, and biocompatibility.[1] Its versatility as a component in membranes has been utilized, for example, for the immobilization of proteins[2] and the separation of enantiomeric molecules.[3] Natural celluloses (e.g. cotton) are complex hierarchical structures composed of crystalline cellulose-I nanofibrils[4] as the fundamental building block.[5] These nanofibrils are typically 4−20 nm in diameter and several hundred nanometers long, and they can be obtained in the form of stable colloidal solutions in water.[6] There has been considerable recent interest in extracting cellulose nanofibrils from natural sources in order to reconstitute materials which mimic or even supersede natural celluloses for applications in textiles[7] and biocomposites.[8,9] The self-assembly of cellulose nanofibrils into new structures has been highlighted as an important development,[10] and recently we have demonstrated that negatively charged cellulose nanofibril building blocks in aqueous solution are readily combined (in a layer-by-layer assembly process) with positively charged titania nanoparticles[11] into extremely thin mesoporous films with interesting electrical properties and the ability to absorb redox proteins.

The selective adsorption and release of analytes at modified electrode surfaces is important for sensing applications and, in particular, for the direct determination of low-concentration targets in complex matrices.[12] Modified electrodes have been commonly used, for example, for the determination of trace mercury,[13] dopamine,[14] glucose,[15] and DNA.[16] Here, the application of cellulose composite films reconstituted onto the electrode surface is considered as a novel approach to produce selective and potentially bio-compatible sensor films with high selectivity. The reconstitution of a cellulose "backbone" together with suitable "receptor" molecules such as poly(diallyldimethylammonium chloride) introduces selectivity toward anions and, in particular, toward hydrophobic anions. These anions can be effectively extracted from aqueous solution into cationic binding sites and then determined with a voltammetric technique.

In this study, both reconstituted cellulose and cellulose−PDDAC film electrodes are characterized and redox processes

* Corresponding author. E-mail: F.Marken@bath.ac.uk.
[†] Department of Chemistry, University of Bath.
[‡] Department of Physics, University of Bath.
[§] Technical University of Crete.
[||] Unilever Research & Development Port Sunlight.
[⊥] University of Nottingham.

10.1021/jp709783k CCC: $40.75
Published on Web 01/31/2008

within these films are investigated. The principle of embedding the "receptor" into the cellulose "backbone" is demonstrated, and model redox systems such as $Fe(CN)_6^{3-/4-}$ and triclosan are employed to investigate the binding ability, film composition effects, and diffusion effects. The potential benefits of cellulose nanocomposite films in analytical processes are evaluated.

2. Experimental Section

2.1. Reagents. KCl, $K_3Fe(CN)_6$, $K_4Fe(CN)_6$, poly(diallyldimethylammonium chloride) (PDDAC, very low molecular weight, 35 wt % in water), and potassium phosphate (monobasic) were obtained from Aldrich and used without further purification. Triclosan (2,4,4′-trichloro-2′-hydroxydiphenyl ether or Irgasan) was obtained from Fluka. Cellulose nanofibrils (0.69 wt % solutions in water) were prepared from sisal following a literature procedure.[17] Demineralized and filtered water was taken from an Elgastat water purification system (Elga, High Wycombe, Bucks) with a resistivity of not less than 18 MΩ cm.

2.2. Instrumentation. For voltammetric studies, a microAutolab II potentiostat system (EcoChemie, NL) was employed with a Pt gauze counter electrode and a saturated calomel (SCE) reference electrode (REF401, Radiometer, Copenhagen). The working electrode was a 3 mm diameter glassy carbon electrode (BAS, US). Experiments were conducted after deaerating with high-purity argon (BOC) for at least 15 min prior to recording voltammograms. The temperature during experiments was 20 ± 2 °C.

Raman spectroscopy studies were carried out with a Renishaw Raman microscope system with a resolution of about 2 cm^{-1} and using an excitation energy of 5.08 eV (244 nm) provided by a frequency-doubled continuous-wave argon ion laser. FTIR spectra were obtained with Nicolet Protégé 460 FTIR spectrometer employing KBr pellets. For surface topography imaging, an atomic force microscope (Digital Instruments Nanoscope III, used in contact mode) was employed. Field emission gun scanning electron microscopy (FEGSEM) images were obtained using a Leo 1530 system. Samples were gold-sputter-coated to improve the image quality. A SAXS/WAXS (simultaneous small-angle X-ray scattering and wide-angle X-ray scattering) pattern of cellulose films was obtained on a SAXSess system using a PW3830 X-ray generator. The X-ray image plates were observed using a Perkin-Elmer Cyclone Storage Phosphor System. The wide-angle patterns were recorded with Cu Kα radiation ($\lambda = 1.5406$ Å) at 40 kV and 50 mA in the region of 2θ from 5° to 25° with an exposure time of 45 min while simultaneously recording small-angle patterns in the region of 0.2−100 Å. Elemental C, H, N, Cl microanalysis was carried out at the Department of Chemistry Services at Bristol University. Fe elemental microanalysis was carried out in house by digestion in nitric acid and AAS detection.

2.3. Reconstitution of Cellulose and Cellulose Nanocomposite Films. For reconstitution of a plain cellulose film, a 5 μL solution of 0.69 wt % cellulose nanofibrils was deposited onto a 3 mm diameter glassy carbon electrode (BAS), placed upright in a holder, and kept in an oven at 60 °C for 20 min. The resulting 30 μg film deposit was approximately 1.5 to 2.0 μm thick (vide infra) and remained intact upon immersion in aqueous electrolyte media. In order to form cellulose−PDDAC composite films, an appropriate amount of poly(diallyldimethylammonium chloride) (PDDAC) solution was added in the cellulose solution, vigorous stirring (ultrasonication) was applied, and the resulting mixture was then used for deposition processes. The same evaporation conditions were employed. Typically, a solution of 0.46 wt % cellulose nanofibrils and 0.12 wt % PDDA was used to create cellulose−PDDAC composite films with about 80 wt % cellulose and about 20 wt % PDDAC.

Free-standing films were required for SAXS/WAXS and elemental microanalysis. These films were prepared from 1 mL of deposition solution on a flat Teflon substrate (area ca. 2 cm^2), placed in an oven at 60 °C for 1 h, and peeled off the Teflon surface with a pair of tweezers. The films were then left to equilibrate at ambient temperature and humidity.

3. Results and Discussion

3.1. Reconstitution of Cellulose and Cellulose−PDDAC Films at Electrode Surfaces. To form thin cellulose films, a solvent evaporation technique was employed (see Experimental Section). Evaporation of an aqueous 0.69 wt % solution of cellulose nanofibrils (5 μL) onto glass or glassy carbon electrode surfaces (ca. 7×10^{-6} m^2 area) resulted in a uniform and stable film coating. During the drying process, bonds (predominantly hydrogen bonds) between randomly packed cellulose nanofibrils developed and the resulting structure remained intact even when re-immersed into aqueous electrolyte solutions. An AFM image of a typical cellulose film (with a scratch revealing the bare substrate on the right) is shown in Figure 1A. Individual cellulose nanofibrils can be seen to pack densely. From the topography height information (not shown), the approximate thickness of this kind of film can be estimated as about 1.5 to 2.0 μm.

The properties of the reconstituted cellulose film can be controlled by nanocomposite formation, for example, with polyelectrolytes. Here, poly(diallyldimethylammonium chloride) (or PDDAC) polycationomer is mixed into the cellulose nanofibril sol and evaporation of the mixture then leads to modified cellulose films. A typical SEM image of this kind of film is shown in Figure 1B. It can be seen that a highly uniform deposit composed predominantly of nanofibrils is formed. At high magnification, again individual nanofibrils and pores are visible typically with up to 10 nm diameter.

Raman spectroscopy, in particular when obtained with a short wave length UV-laser is a powerful tool for the investigation of the cellulose structures.[18] A Raman spectrum obtained with a confocal microscopy system (excitation wavelength 244 nm) for a cellulose nanofibril film deposit and a FTIR spectrum for a KBr pellet (see Figure 1C, bottom and top, respectively) reveal characteristic absorption bands for the cellulose-I structures. The absorption band A at 3250 cm^{-1} can be attributed to OH-stretching of hydroxyl groups in the cellulose chain,[19] while the absorption bands at B, D, and E are due to CH-stretching[20] and -bending modes, respectively, in the cellulose chain. The strong additional band C at 1640 cm^{-1} is believed to be inherently linked to the cellulose backbone interaction with absorbed water molecules in the structure and has also been observed for other polysaccharides.[21]

In order to obtain elemental analyses for cellulose and cellulose−PDDAC films, free-standing films were required. When cast onto Teflon-coated surfaces and dried at 60 °C, the cellulose sol allows thicker free-standing cellulose films to be formed and peeled off intact. Similar films can be readily formed for cellulose−PDDAC and post-treated, for example, by soaking in aqueous solution. A plain free-standing cellulose film is optically almost transparent. However, upon the incorporation of PDDAC, films become more opaque probably due to more heterogeneity within the structure. Next, the elemental composition of the cellulose films was studied using microanalysis. For a plain free-standing cellulose film (formed by the deposition

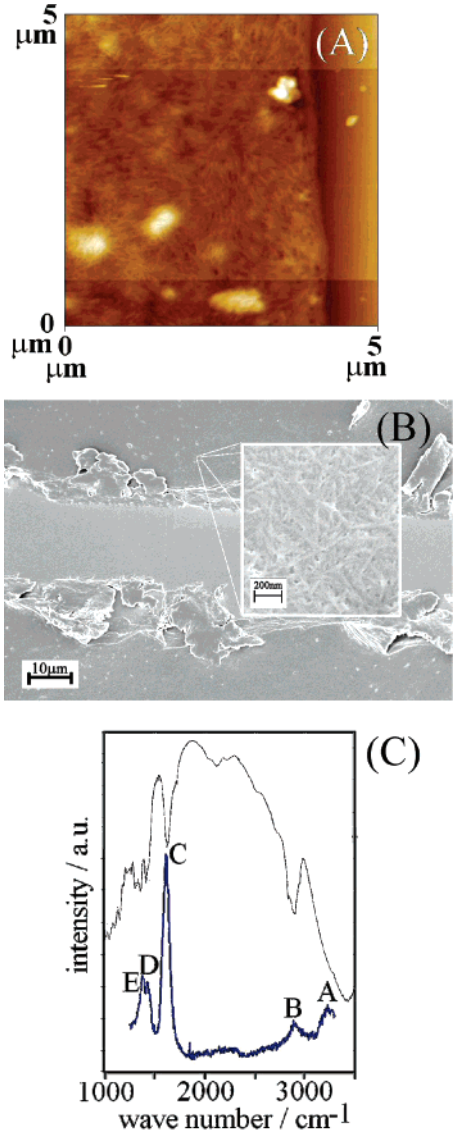

Figure 1. (A) AFM image for a cellulose nanofibril film showing individual nanofibrils packed into a dense layer of approximately 1.5−2.0 μm thickness. A scratch on the right reveals the substrate. (B) Field emission gun scanning electron microscopy (FEGSEM) images for a co-deposited film of cellulose nanofibril (80 wt %) and PDDAC (20 wt %) on a glass surface. A scratch was applied to investigate the mechanical properties of the film. The inset shows a magnified region with individual cellulose nanofibrils and pores. A gold sputter coating was applied prior to imaging. (C) FTIR adsorption (obtained with KBr pellet, top) and confocal Raman (bottom, $\lambda = 244$ nm) obtained for a cellulose nanofibril film.

of 0.69 wt % cellulose nanofibril solution), the elemental composition was determined as 41.55% C (theoretical 44.44% without H_2O) and 6.09% H (theoretical 6.22% without H_2O) with zero nitrogen content. A good match for C and H was observed when taking into account the presence of about 0.6 equiv H_2O per cellulose monomer. Upon modification of the film (by changing the deposition solution composition) to 80 wt % cellulose nanofibrils and 20 wt % PDDACl (equilibrated in 0.1 M phosphate buffer pH 9.5 for 10 min), the film elemental composition changed to 41.26% C, 6.50% H, 1.49% N, and 3.70% Cl. The theoretical elemental composition assuming 1.3 H_2O per formula weight is 41.45% C, 7.50% H, 1.51% N, and 3.82% Cl, in good agreement with the measured values. The increase in water content is likely to result from the more hydrophilic nature of PDDAC polyelectrolyte.

The elemental analysis for nitrogen provides a convenient measure for cationic binding sites in the cellulose−PDDAC film deposits on electrode surfaces. A content of 1.49% N in approximately 30 μg film corresponds to about 30 nmol cationic binding sites (or formally a concentration of ca. 2 mol dm^{-3} within the film). Some of these cationic sites are responsible for binding to the sulfate half-ester groups on the cellulose surface (vide infra).

3.2. Small- and Wide-Angle X-ray Scattering Studies of Reconstituted Cellulose and Cellulose−PDDAC Films. X-ray scattering techniques offer a powerful probe into both the atomic and nanostructure of composite materials.[22] Previous studies of cellulose nanofibril materials have shown that the nanofibrils usually have a ribbonlike morphology.[23] Here, the morphologies of both cellulose and cellulose−PDDAC composite films were investigated with wide- and small-angle X-ray scattering techniques, and the ribbon morphology is confirmed.

In Figure 2A, the small-angle X-ray scattering pattern for a nanocellulose film and a nanocellulose−PDDAC modified film (80 wt % cellulose and 20 wt % PDDAC) are shown. A direct relationship between the scattering intensity, I, and the value of the momentum transfer, Q (which is given by $Q = 4\pi/(\lambda \sin \theta)$, where θ is half the scattering angle), is observed. A high degree of polydispersity is manifest by the lack of any well-defined peaks in the scattering pattern. The small-angle scattering analysis package written by "The SANS Group" at NIST for the Igor Pro platform was used to determine the geometry and consequent dimensions of the particles in the plain nanocellulose film. When testing different models, it was found that a theoretical ribbon (parallelepiped) scattering pattern gave the best match between experiment and simulation (red line, Figure 2A). This result is consistent with recent work by Celine Bonini et al.[24] on similar cellulose nanofibril structures. For the best-fitting model using a monodisperse parallelepiped, the rectangular cross-section of the ribbon had average dimensions of approximately 2.4 nm × 23 nm (see Figure 2A). In this case, not considering polydispersity severely limits the accuracy of the fit of experimental data, the published TEM data (3 to 5 nm ribbon diameter and ca. 250 nm length[17]) are believed to be more accurate. Other factors used in the simulation were a background of 1110 au, a contrast setting of 1.46×10^{-5} $Å^{-2}$ (calculated from the monomeric formula of cellulose, $C_6H_{10}O_5$, and a crystal density of 1.62 kg m^{-3}), and a scale factor of 29.0197. The polydisperse ribbon structure is consistent with the appearance of AFM and SEM images (see Figure 1) and likely to result from the hydrogen bonding in crystalline cellulose-I.

Upon the introduction of PDDAC into the cellulose film, an additional feature is observed in the scattering pattern (see green dots in Figure 2A) at about 1.2 nm^{-1}. This feature suggests an interaction of the polymer with the cellulose. Using the relationship $d = 2\pi/Q$, this feature corresponds to a repeat distance of approximately 5.2 nm—slightly more than the width of the ribbons in the plain cellulose samples. This indicates that a thin polymer layer is present between two cellulose ribbons (very much like a "sandwich" structure). It was not possible to fit this pattern using the same ribbon model as used for plain cellulose, suggesting that a higher-order structure exists in this sample.

Next, Guinier analysis was applied to the experimental curves of both films. A good linearity (see Figure 2B) is observed in the range 4×10^{-2} $nm^{-2} < Q^2 < 1.2 \times 10^{-1}$ nm^{-2} (the Guinier condition, $QR_G < 1$ applies in this range). The measured slope

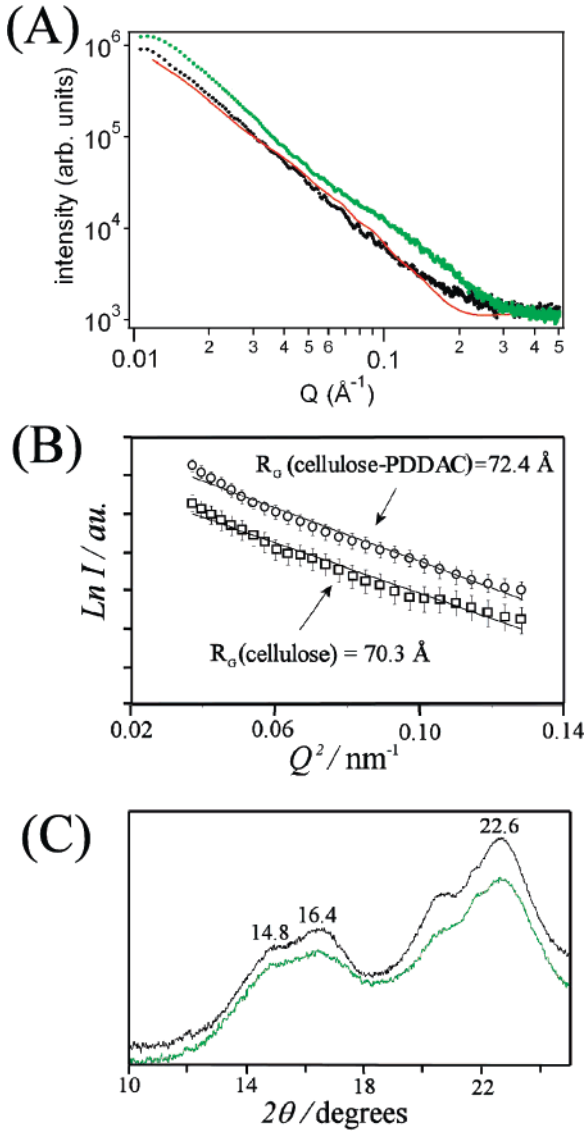

Figure 2. (A) Small-angle X-ray scattering pattern for nanocellulose films reconstituted from an aqueous 0.69 wt % cellulose nanofibril solution (black dots) and reconstituted from aqueous 0.46 wt % cellulose nanofibrils and 0.12 wt % PDDAC (green dots). The red line is a simulated fit of a parallelepiped or ribbon-based scattering pattern with (24 ± 0.2 Å) × (233 ± 18 Å nm) × (1300 ± 70 Å) ribbon dimensions (assuming monodispersity, see text). (B) A Guinier plot of the natural logarithm of intensity, ln *I*, versus the momentum transfer squared, Q^2, measured for nanocellulose films reconstituted from aqueous 0.69 wt % cellulose nanofibril solution (squares) and from 0.46 wt % cellulose nanofibrils and 0.12 wt % PDDAC (circles) both with a similar radius of gyration, $R_G \approx 7$ nm. (C) Wide-angle X-ray scattering pattern for nanocellulose films reconstituted from aqueous 0.69 wt % cellulose nanofibril solution (black line) and from 0.46 wt % cellulose nanofibrils and 0.12 wt % PDDAC (green line). Numbers indicate characteristics lines for the cellulose-I structure.

can be used to extract particle size information based on eq 1:[25]

$$\ln I = \ln I_0 - \left(\frac{R_G^2}{3}\right)Q^2 \qquad (1)$$

where R_G is the radius of gyration. The addition of the polymer increased the radius of gyration slightly. The measured values are for the plain nanocellulose film, $R_G = 70.3$ Å, and for the cellulose−PDDAC film, $R_G = 72.4$ Å. The magnitude of R_G when compared to the aspect ratio predicted by the simulation

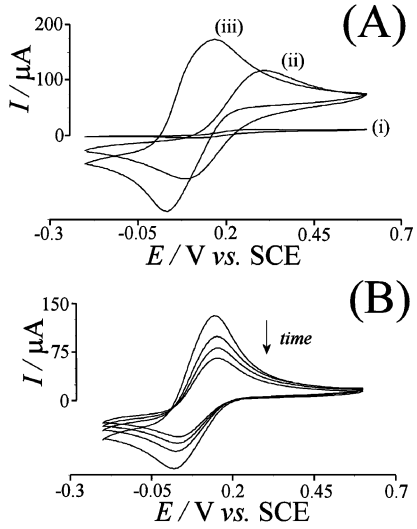

Figure 3. (A) Cyclic voltammograms (second scan shown, scan rate 100 mV s^{-1}) for the oxidation and re-reduction of 1 mM ferrocyanide in aqueous 0.1 M KCl at (i) a cellulose nanofibril modified electrode, (ii) a bare glassy carbon electrode, and (iii) a cellulose−PPDAC film (80 wt % cellulose, 20 wt % PDDAC) modified glassy carbon electrode (3 mm diameter). (B) Cyclic voltammograms (second scan shown, scan rate 100 mV s^{-1}) for the oxidation and re-reduction of $Fe(CN)_6^{4-}$ (immobilized in a cellulose−PPDAC film with 80 wt % cellulose and 20 wt % PDDAC at a glassy carbon electrode after soaking in 1 mM $Fe(CN)_6^{4-}$ in 0.1 M KCl for 15 min) immersed into 0.1 M KCl and measured periodically (data shown for 5, 10, 15, and 20 min immersion).

suggests that the ribbon structure is bundled and only slightly expanded. The slight R_G increase for the cellulose−PDDAC film seems reasonable in the context of the ribbon morphology.

In the wide-angle X-ray scattering pattern (see Figure 2C), a classic cellulose pattern is observed for both the plain cellulose and the cellulose−PDDAC films. The data are consistent with scattering by the cellulose-I polymorph,[26] where the intensity peak at 14.8° is caused by scattering from the $1\bar{1}0$ diffraction plane, 16.4° from the 110 diffraction plane, and 22.6° by the 020 diffraction plane. The additional peak found in the pattern at 20.6° (shoulder) could be due to a small amount of the polymorphic variation cellulose-III structure, which is commonly seen in reconstituted forms of cellulose.

The structural characterization of the cellulose−PDDAC film clearly suggests a highly distributed PDDAC polycation in a cellulose backbone. The "sandwich" structure should open up an extended network of nanopores where anions can penetrate the film and accumulation of anions (by ion exchange) as well as propagation (by diffusion) throughout the film is anticipated. In order to explore the properties and reactivity of cellulose−PDDAC films, electrochemical studies are reported next.

3.3. Electrochemical Processes in Reconstituted Cellulose and Cellulose−PDDAC Films. *3.3.1. The $Fe(CN)_6^{3-/4-}$ Redox System.* Electrochemical experiments at electrodes modified with thin films give access to quantitative data on ion permeability and adsorption effects. Here, both cellulose and cellulose−PDDAC films were investigated in aqueous 0.1 M KCl employing the $Fe(CN)_6^{3-/4-}$ redox system. A film of cellulose nanofibrils (from 5 μL 0.69 wt % solution deposited onto a 3 mm diameter glassy carbon electrode) has a strong effect on the appearance of voltammograms for the oxidation of $Fe(CN)_6^{4-}$ (see Figure 3A). In the absence of the cellulose film, a well-defined voltammetric response (curve ii) is observed with a reversible potential of about 0.21 V vs SCE. This process is

consistent with the one-electron redox system $Fe(CN)_6^{4-/3-}$ (eq 2):

$$Fe(CN)_6^{4-}(aq) \rightleftarrows Fe(CN)_6^{3-}(aq) + e^- \qquad (2)$$

The cellulose nanofibril film without PDDAC has a very strong blocking effect which reduces the peak current by about 95% (see curve i). The remaining current response appears at the same potential and is believed to be due to a pinhole effect where bigger pores (see Figure 1) allow some $Fe(CN)_6^{4-}$ to diffuse into the film and to the electrode surface.

Next, poly(diallyldimethylammonium chloride) or PDDAC embedded into the cellulose film was investigated. Curve iii in Figure 3A shows that in the presence of a film of 80 wt % cellulose and 20 wt % PDDAC the peak current for the oxidation of $Fe(CN)_6^{4-}$ is substantially increased and the reversible potential is shifted negative to about 0.11 V vs SCE. The potential shift[27] and appearance of the peak are consistent with a one-electron transfer within the cellulose−PDDAC membrane (eq 3):

$$Fe(CN)_6^{4-}(mem) \rightleftarrows Fe(CN)_6^{3-}(mem) + e^- \qquad (3)$$

To explore the accumulation and reactivity of $Fe(CN)_6^{4-}$ in a cellulose−PDDAC film in more detail, the modified glassy carbon electrode was pretreated by immersion into a solution of 1 mM $Fe(CN)_6^{4-}$ in 0.1 M KCl and then rinsed and transferred into clean aqueous 0.1 M KCl. Figure 3B shows that under these conditions a similar response was obtained and that only a very slow loss of the voltammetric signal occurs (ca. 50% over 30 min) consistent with a high partitioning coefficient and strong binding of the $Fe(CN)_6^{4-}$ anion into the film and/ or slow diffusion (vide infra).

The effect of the scan rate on the voltammetric response is shown in Figure 4, parts A and B. The process, although complex in peak shape, follows the trend expected for a diffusion-controlled process over a range of scan rates from 200 to 10 mV s^{-1}. Therefore diffusion within the cellulose−PDDAC film is dominating the transport process (probably associated with both diffusion of anions along polycationomer "sandwich" domains and charge transport via electron hopping). The binding of $Fe(CN)_6^{4-}$ into the cellulose−PDDAC film is concentration-dependent with an isotherm at least approximately consistent with Langmuirian characteristics (see Figure 4C, note that diffusion effects may cause deviations from ideal behavior). The approximate binding constant $K = 12000$ mol^{-1} dm^3 is observed in aqueous 0.1 M KCl.

The effect of PDDAC content on the film behavior can be monitored electrochemically (Figure 5). As the amount of PDDAC increases, so does the current response seen in the cyclic voltammetry (Figure 5A). This can, in turn, be correlated to the number of ferrocyanide anions present in the film at the electrode surface, by integrating the anodic peak current. The corresponding plot (see Figure 5B) shows a monotonic but nonlinear increase which is believed to be associated with the concomitant increase in both the bound $Fe(CN)_6^{4-}$ concentration and mobility (or diffusivity).

Next, the characteristics for accumulation and reactivity of $Fe(CN)_6^{3-}$ are contrasted with those observed for $Fe(CN)_6^{4-}$ (see Figure 6). Due to the lower charge of $Fe(CN)_6^{3-}$ compared to that of $Fe(CN)_6^{4-}$ the initial peak currents (and charge under the voltammetric response) are increased by approximately 25% (assuming the same number of cationic binding sites in the cellulose−PDDAC film).

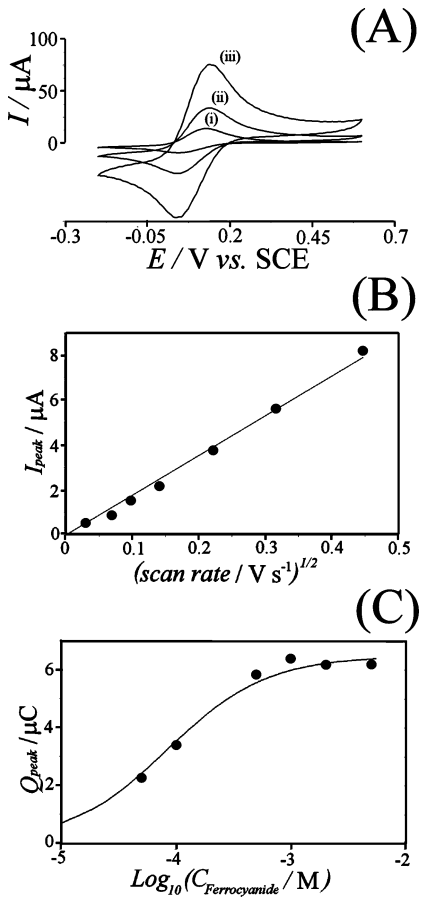

Figure 4. (A) Cyclic voltammograms (second scan shown) for the oxidation and re-reduction of $Fe(CN)_6^{4-}$ (immobilized by soaking in a 1 mM $Fe(CN)_6^{4-}$ in 0.1 M KCl for 15 min) at a cellulose−PDDAC modified electrode (80 wt % cellulose and 20 wt % PDDAC) immersed in 0.1 M KCl. (B) Plot of the change of peak current (I_{peak}) versus the square root of the scan rate for the oxidation of ferrocyanide in a cellulose−PDDAC film modified electrode (80 wt % cellulose and 20 wt % PDDAC) immersed in 0.1 M KCl. (C) Langmuir isotherm plot for the immobilization of varying amounts of $Fe(CN)_6^{4-}$ (from a 0.1 M KCl solution) into a cellulose−PDDAC film. The approximate binding constant is $K = 12000$ mol^{-1} $dm.^3$

The total number of binding sites within the cellulose−PDDAC film has been investigated by elemental analysis. On the basis of the nitrogen content (vide supra) in a film composed of 80 wt % cellulose and 20 wt % PDDAC, approximately 30×10^{-9} mol binding sites should be available within the film deposit. The iron content in cellulose−PDDAC films soaked in $Fe(CN)_6^{4-}$ was investigated by elemental analysis for 1, 5, and 10 mM solutions (all corresponding to fully saturated binding sites, see Figure 4C). Consistently a constant iron content of about 0.5% was determined which indicates that in total about 2.7×10^{-9} mol $Fe(CN)_6^{4-}$ are present at the cellulose−PDDAC modified electrode. Taking into account the 4-fold negatively charged nature of the anion, this result suggests that approximately 30% of the available anion binding sites are occupied by $Fe(CN)_6^{4-}$. This result appears very realistic given that some of the cationic sites are required to bind to or compensate the negative surface charges of the cellulose nanofibrils. It is interesting to compare the total iron content of 2.7×10^{-9} mol (or 260 μC charge) with the charge under voltammetric experiments with immobilized $Fe(CN)_6^{3-/4-}$ (typically 10 μC). It is obvious that only a very thin layer of the film (ca. 5% or 75 to 100 nm) adjacent to the electrode is active. Accordingly, the apparent diffusion coefficient for the

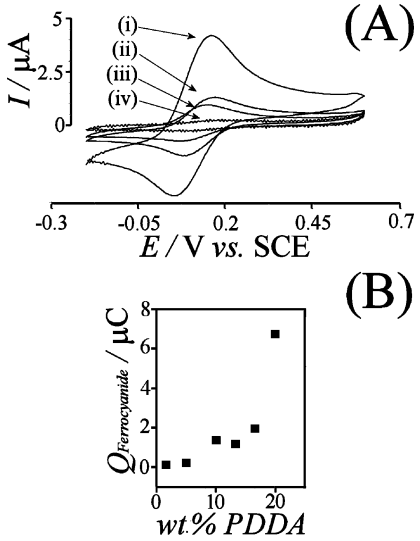

Figure 5. (A) Cyclic voltammograms (second scan, scan rate 100 mV s^{-1}) for the oxidation and re-reduction of $Fe(CN)_6^{4-}$ immobilized (soaked in 1 mM $Fe(CN)_6^{4-}$ in 0.1 M KCl for 15 min) into cellulose−PDDAC films with varying compositions ((i) 20, (ii) 18, (iii) 15, and (iv) 6 wt % PDDAC) at a 3 mm diameter glassy carbon electrode immersed in 0.1 M KCl. (B) Plot of the change in charge under the oxidative peak ($Q_{Ferrocyanide}$) versus wt % content of PDDAC in the film at the electrode surface.

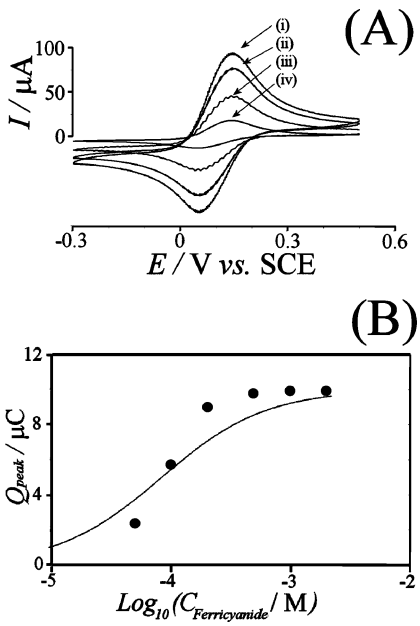

Figure 6. (A) Cyclic voltammograms (second scan shown) for the reduction and re-oxidation of $Fe(CN)_6^{3-}$ (immobilized from 1 mM $Fe(CN)_6^{3-}$ in 0.1 M KCl for 15 min) in a cellulose−PDDAC film (80 wt % cellulose−20 wt % PDDAC) immersed in 0.1 M KCl with varying scan rates of (i) 200, (ii) 100, (iii) 50, and (iv) 10 mV s^{-1}. (B) Langmuir isotherm plot for the charge under the reduction signal versus the concentration of $Fe(CN)_6^{3-}$ during immobilization. The line shows the expected behavior for a binding constant $K = 12000$ mol^{-1} $dm.^3$

$Fe(CN)_6^{3-/4-}$ redox system (which includes actual diffusion as well as electron-hopping transport contributions) is in the order of 10^{-15} m^2 s^{-1} (or 6 orders of magnitude lower in the cellulose−PDDAC membrane than in aqueous solution[28]). This is only a crude estimate and it is likely that under these conditions, the diffusion coefficients for $Fe(CN)_6^{4-}$ and $Fe(CN)_6^{3-}$ are not equal and concentration-dependent.

3.3.2. The Accumulation and Oxidation of Triclosan. Triclosan (or 2,4,4′-trichloro-2′-hydroxydiphenyl ether) is a polychlorinated aromatic phenol which is poorly water soluble (in neutral media) and widely used as biocide. As a phenol, it is readily oxidized and the anodic peak current observed in voltammetric measurements has been employed for the quantitative determination at mercury electrodes,[29] at carbon microfibers,[30] and at screen-printed electrodes.[31] The hydrophobic nature of the triclosan anion has been exploited recently for the accumulation and detection in carbon−PDDAC thin-film electrodes.[32]

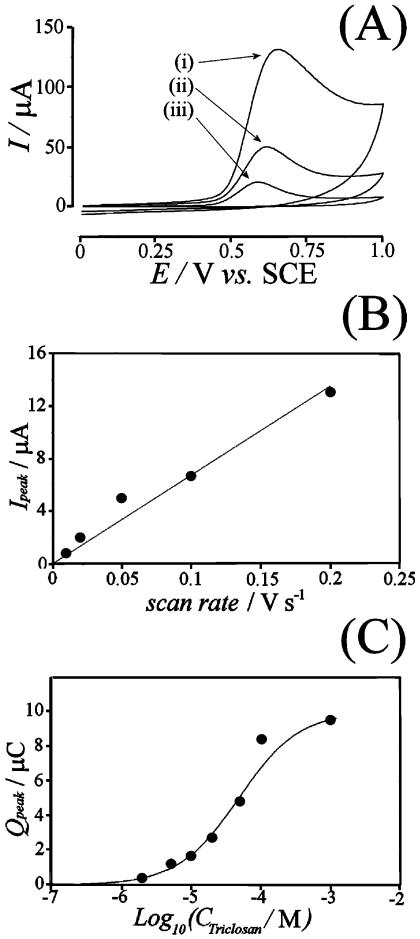

Figure 7. (A) Cyclic voltammograms (first scan shown) for the oxidation of triclosan (immobilized into a 80 wt %−20 wt % cellulose−PPDAC film at a 3 mm diameter glassy carbon electrode by soaking in 1 mM triclosan in 0.1 M phosphate buffer pH 9.5 for 15 min) immersed in 0.1 M phosphate buffer pH 9.5 with a scan rate of (i) 200, (ii) 50, and (iii) 10 mV s^{-1}. (B) Plot of the peak current (I_{peak}) versus the scan rate for the oxidation of triclosan (immobilized as in (A)) in a cellulose−PDDAC film immersed in 0.1 M phosphate buffer pH 9.5. (C) Langmuir isotherm plot for the immobilization of varying amounts of triclosan (immobilized as in (A)) in a cellulose−PDDAC film. The line indicates the theoretical curve for the binding constant $K = 21000$ mol^{-1} $dm.^3$

Figure 7 shows typical voltammetric data for the oxidation of triclosan immobilized (from a solution in 0.1 phosphate buffer pH 9.5) into a cellulose−PDDAC film (80 wt % cellulose 20 wt % PDDAC). In the absence of PDDAC, no oxidation of triclosan occurs and therefore the positive binding sites in the PDDAC component are crucial.

The oxidation of triclosan is chemically irreversible and believed to lead to radical intermediates and oligomeric products[33] similar to polyoxyphenylenes formed during phenol oxidation (eq 4):

The voltammetric response for the oxidation is dependent on the scan rate (see Figure 7, parts A and B), and the peak current

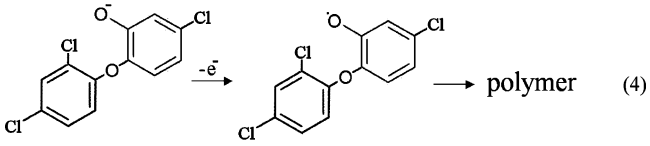

(4)

appears to be increasing approximately linearly with scan rate. The reason for the linear dependence (in contrast to the characteristics observed for $Fe(CN)_6^{3-/4-}$ in Figure 4) is likely to be the irreversible formation of products which is limiting the diffusion of more reagent from the bulk of the cellulose−PDDAC film toward the electrode and suppressing any contributions from electron-hopping transport. The detection of varying concentrations of triclosan is demonstrated in Figure 7C. Lower concentrations down into the micromolar level are easily detected, and the binding of triclosan can be well approximated by a Langmuirian relationship with a binding constant $K = 21000$ mol^{-1} dm^3.

4. Conclusions

It has been shown that reconstituted cellulose and cellulose−PDDAC films exhibit an interesting ribbon structure where "receptors" such as polycationic PDDAC can be embedded in a "sandwich" structure to provide selective binding sites for the accumulation and transport of multiply charged or hydrophobic anions such as $Fe(CN)_6^{3-/4-}$ or triclosan. Voltammetric studies show that, although diffusion within the cellulose−PDDAC structure is slow (ca. 6 orders of magnitude slower than in aqueous solution), good analytical signals are obtained and hydrophobic anionic impurities such as triclosan can be accumulated and detected down to a 10^{-6} mol dm^{-3} level. The versatility of cellulose and the facile incorporation of "receptor" components into nanocellulose films will be of interest in many areas of sensor development, membrane technology, and drug-release applications.

Acknowledgment. W.T. thanks EPSRC for funding under the Driving Innovation in Chemistry and Chemical Engineering (DICE) Science and Innovation Award (Grant Number EP/D501229/1). M.J.B. thanks Unilever Research & Development Port Sunlight for a PhD stipend and support. F.M. and E.P. thank the British Council for the award of a scientific exchange project entitled "Novel Environmental Technologies".

References and Notes

(1) Klemm, D.; Schumann, D.; Kramer, F.; Hessler, N.; Hornung, M.; Schmauder, H. P.; Marsch, S. *Polysaccharides II. Adv. Polym. Sci.* **2006**, *205*, 49.

(2) Martinez, A. J.; Manolache, S.; Gonzalez, V.; Young, R. A.; Denes, F. J. *J. Biomater. Sci., Polym. Ed.* **2000**, *11*, 415.

(3) Götmar, G.; Zhou, D.; Stanley, B. J.; Guiochon, G. *Anal. Chem.* **2004**, *76*, 197.

(4) Krässig, H. A. *Cellulose, Structure, Accessibility, and Reactivity*; Gordon and Breach: Amsterdam, 1996.

(5) Klemm, D.; Heublein, B.; Fink, H. P.; Bohn, A. *Angew. Chem., Int. Ed.* **2005**, *44*, 3358.

(6) Beck-Candanedo, S.; Roman, M.; Gray, D. G. *Biomacromolecules* **2005**, *6*, 1048.

(7) *Regenerated cellulose fibers*; Woodings, C., Ed.; Woodhead Publishing Ltd.: Cambridge, UK, 2001.

(8) Samir, M. A. S. A.; Alloin, F.; Dufresne, A. *Biomacromolecules* **2005**, *6*, 612.

(9) Linder, A. P.; Bergman, R.; Bodin, A.; Gatenholm, P. *Langmuir* **2003**, *19*, 5072.

(10) Oksman, K.; Sain, M. *Cellulose nanocomposites, processing, characterization and properties*; ACS Symp. Ser. 938; American Chemical Society: Washington, DC, 2005.

(11) Bonné, M. J.; Milsom, E. V.; Helton, M.; Thielemans, W.; Wilkins, S.; Marken, F. *Electrochem. Commun.* **2007**, *9*, 1985.

(12) Logrieco, A.; Arrigan, D. W. M.; Brengel-Pesce, K.; Siciliano, P.; Tothill, I. *Food Addit. Contam.* **2005**, *22*, 335.

(13) Dias, N. L.; Caetano, L.; do Carmo, D. R.; Rosa, A. H. *J. Braz. Chem. Soc.* **2006**, *17*, 473.

(14) Amiri, M.; Shahrokhian, S.; Marken, F. *Electroanalysis* **2007**, *19*, 1032.

(15) Wu, Y. H.; Hu, S. S. *Microchim. Acta* **2007**, *159*, 1.

(16) He, P. A.; Xu, Y.; Fang, Y. Z. *Anal. Lett.* **2005**, *38*, 2597.

(17) Garcia de Rodriguez, N. L.; Thielemans, W.; Dufresne, A. *Cellulose* **2006**, *13*, 261.

(18) Österberg, M.; Schmidt, U.; Jääskeläinen, A. A. *Colloids Surf., A* **2006**, *291*, 197.

(19) Michell, A. J. *Carbohydr. Res.* **1988**, *173*, 185.

(20) Michell, A. J. *Carbohydr. Res.* **1993**, *241*, 47.

(21) Barker, S. A. In *Methods in Carbohydrate Chemistry, Vol. III: Cellulose*; Whistler, R. L., Wolfrom, M. L., Eds.; Academic Press: New York, 1962; p 104.

(22) *Small Angle X-ray Scattering*; Glatter, O., Kratky, O., Eds.; Academic Press: New York, 1982.

(23) Terech, P.; Chazeau, L.; Cavaille, J. Y. *Macromolecules* **1999**, *32*, 1872.

(24) Bonini, C.; Heux, L.; Cavaille, J. Y.; Lindner, P.; Dewhurst, C.; Terech, P. *Langmuir* **2002**, *18*, 3311.

(25) Hosemann, R.; Bagchi, S. N. *Direct Analysis of Diffraction by Matter*; North Holland Publishing Co.: Amsterdam, The Netherlands, 1962; 734 pp.

(26) Isogai, A.; Usuda, M.; Kato, T.; Uryu, T.; Atalla, R. H. *Macromolecules* **1989**, *22*, 3168.

(27) McKenzie, K. J.; King, P. M.; Marken, F.; Gardner, C. E.; Macpherson, J. V. *J. Electroanal. Chem.* **2005**, *579*, 267.

(28) Adams, R. N. *Electrochemistry at solid electrodes*; Marcel Dekker: New York, 1969; p 220.

(29) Safavi, A.; Maleki, N.; Shahbaazi, H. R. *Anal. Chim. Acta* **2003**, *494*, 225.

(30) Wang, L. H.; Chu, S. C.; Chin, C. Y. *Bull. Electrochem.* **2004**, *20*, 225.

(31) Pemberton, R. M.; Hart, J. P. *Anal. Chim. Acta* **1999**, *390*, 107.

(32) Amiri, M.; Shahrokhian, S.; Psillakis, E.; Marken, F. *Anal. Chim. Acta* **2007**, *593*, 117.

(33) Ghanem, M. A.; Compton, R. G.; Coles, B. A.; Psillakis, E.; Kulandainathan, M. A.; Marken, F. *Electrochim. Acta* **2007**, doi:10.1016/j.electacta.2007.01.065.